Published in final edited form as:
Synapse. 2012 June ; 66(6): 471–482. doi:10.1002/syn.21515.

Correlation of the Vesicular Acetylcholine Transporter Densities in the Striata to the Clinical Abilities of Women with Rett Syndrome (RTT)

JAMES ROBERT BRAŠIĆ[1], **GENILA BIBAT**[2,3], **ANIL KUMAR**[1], **YUN ZHOU**[1], **JOHN HILTON**[1], **MARYBETH E. YABLONSKI**[3], **AHMET SEMIH DOGAN**[1], **MARIA RITA GUEVARA**[1], **MASSOUD STEPHANE**[1], **MICHAEL JOHNSTON**[2,4,5,6], **DEAN FOSTER WONG**[1,7,8,9], and **SAKKUBAI NAIDU**[2,3,4,10]

[1]Section of High Resolution Brain Positron Emission Tomography Imaging, Division of Nuclear Medicine, The Russell H. Morgan Department of Radiology and Radiological Science, The Johns Hopkins University School of Medicine, Johns Hopkins Outpatient Center, 601 North Caroline Street, Room 3245, Baltimore, Maryland 21287-0807

[2]Department of Pediatrics, The Johns Hopkins University School of Medicine, Johns Hopkins Outpatient Center, 601 North Caroline Street, Room 3245, Baltimore, Maryland 21287-0807

[3]Neurogenetics Unit, Kennedy Krieger Institute, 801 North Broadway, Baltimore, Maryland 21205

[4]Department of Neurology, The Johns Hopkins University School of Medicine, Johns Hopkins Outpatient Center, 601 North Caroline Street, Room 3245, Baltimore, Maryland 21287-0807

[5]Department of Physical Medicine and Rehabilitation, The Johns Hopkins University School of Medicine, Johns Hopkins Outpatient Center, 601 North Caroline Street, Room 3245, Baltimore, Maryland 21287-0807

[6]Neuroscience Laboratory, Kennedy Krieger Institute, 801 North Broadway, Baltimore, Maryland 21205

[7]Department of Neuroscience, The Johns Hopkins University School of Medicine, Johns Hopkins Outpatient Center, 601 North Caroline Street, Room 3245, Baltimore, Maryland 21287-0807

[8]Department of Psychiatry and Behavioral Sciences, The Johns Hopkins University School of Medicine, Johns Hopkins Outpatient Center, 601 North Caroline Street, Room 3245, Baltimore, Maryland 21287-0807

[9]Department of Environmental Health Sciences, The Johns Hopkins Bloomberg School of Public Health, 615 North Wolfe Street, Baltimore, Maryland 21205

[10]Neurology Laboratory, Kennedy Krieger Institute, 801 North Broadway, Baltimore, Maryland 21205

Correspondence to James Robert Brašić, M.D., M.P.H., Section of High Resolution Brain Positron Emission Tomography Imaging, Division of Nuclear Medicine, The Russell H. Morgan Department of Radiology and Radiological Science, The Johns Hopkins University School of Medicine, Johns Hopkins Outpatient Center, 601 North Caroline Street, Room 3245, Baltimore, MD 21287-0807, telephone 410 955 8354, Facsimile 410 955 0696, brasic@jhmi.edu.

Earlier versions of this manuscript were presented at the 3rd Annual Rett Syndrome Symposium, Rett Syndrome Research Foundation (www.rsrf.org), Baltimore, Maryland, June 17–19, 2002 (Brašić et al., 2002, Chun et al., 2002; Zhou et al., 2002a); the 4th Annual Rett Syndrome Symposium, Rett Syndrome Research Foundation (www.rsrf.org), Baltimore, Maryland, June 23–25, 2003 (Brašić et al., 2003a,b); the 32nd Annual Meeting of the Child Neurology Society, Miami Beach, Florida, October 1–4, 2003 (Bibat et al., 2003); the 56th Annual Meeting of the American Academy of Neurology, San Francisco, California, April 24-May 1, 2004 (Bibat et al., 2004); the 50th Annual Meeting of the Society of Nuclear Medicine, New Orleans, Louisiana, June 21–25, 2003 (Dogan et al., 2003), and the Molecular Neuroimaging Symposium at the Natcher Auditorium, the National Institutes of Health, Bethesda, Maryland, May 6–7, 2010 (Brašić et al., 2010a).

Abstract

Rett syndrome (RTT) is a neurodevelopmental disability characterized by mutations in the X-linked methyl-CpG-binding protein 2 (MeCP2) located at the Xq28 region. The severity is modified in part by X chromosomal inactivation resulting in wide clinical variability. We hypothesized that the ability to perform the activities of daily living (ADL) is correlated with the density of vesicular acetylcholine transporters in the striata of women with RTT. The density of the vesicular acetylcholine transporters in the living human brain can be estimated by single-photon emission-computed tomography (SPECT) after the administration of (−)-5-[^{123}I]iodobenzovesamicol ([^{123}I]IBVM).

Twenty-four (24) hours following the intravenous injection of approximately 333 MBq (9 mCi) [^{123}I]IBVM, four women with RTT and nine healthy adult volunteer control participants underwent SPECT brain scans for sixty (60) minutes. The Vesicular Acetylcholine Transporter Binding Site Index (VATBSI) (Kuhl et al., 1994), a measurement of the density of vesicular acetylcholine transporters, was estimated in the striatum and the reference structure, the cerebellum.

The women with RTT were assessed for certain activities of daily living (ADL). Although striatal VATSBI was not significantly lower in RTT (5.2 ± 0.9) than in healthy adults (5.7 ± 1.6), RTT striatal VATSBI and ADL scores were linearly associated (ADL = 0.89*VATSBI + 4.5; R^2=0.93; $p<0.01$), suggesting a correlation between the ability to perform ADL and the density of vesicular acetylcholine transporters in the striata of women with RTT. [^{123}I]IBVM is a promising tool to characterize the pathophysiological mechanisms of RTT and other neurodevelopmental disabilities.

Keywords

5-iodobenzovesamicol; (−) isomer; ^{123}I-labeled; tomography; emission-computed; single-photon

INTRODUCTION

Rett syndrome (RTT) (Online Mendelian Inheritance in Man (OMIM) 312750) (Hagberg et al., 1983; Rett, 1966) is a developmental disability characterized by mutations in the X-linked methyl-CpG-binding protein 2 (MeCP2) gene [Online Mendelian Inheritance in Man (OMIM) 300005] located at Xq28 (Amir et al., 1999; Sirianni et al., 1998). RTT afflicts 1 in 10,000, to 1 in 20,000 girls (Percy et al., 2007). The disorder is characterized by the deceleration of head growth in infancy, intellectual disabilities, loss of acquired skills in particular the use of the hands, occurrence of stereotyped movements, and progressive rigidity (Naidu, 1997a,b; Naidu et al., 2003). Dysfunction of the MeCP2 gene impedes neuronal maturation, synaptic elaboration, and pruning in childhood (Armstrong, 2001, 2002, 2005; Johnston et al., 2001) which has also been demonstrated in olfactory receptor neurons of girls with RTT (Ronnett et al., 2003). The clinical severity is modified by X chromosome inactivation (XCI) (Bebbington et al., 2008; Hoffbuhr et al., 2001, 2002; Wan et al., 1999; Zoghbi, 2003), and is considered to be skewed when more than 80% of cells reflect a single allele. Nonrandom cases of XCI are often associated with milder or more severe symptoms of RTT (Amir et al., 2000; Amir and Zoghbi, 2000; Hoffbuhr et al., 2002). Although some note that particular mutations of the MeCP2 gene express specific clinical manifestations (Bebbington et al., 2008, 2010; Neul et al., 2008), the basis for variation in clinical severity even within the same mutation is unknown. To understand the basis for the clinical variability (Naidu et al., 2003), we studied the cholinergic system which has been reportedly defective in RTT (Wenk and Hauss-Wegrzyniak, 1999).

Neuroimaging studies demonstrate several differences from controls in RTT. In contrast to healthy normal control subjects, magnetic resonance imaging (MRI) demonstrates (A) decreased volumes of white matter and gray matter of the parietal lobe particularly the dorsal parietal region of girls with RTT and (B) reduced anterior frontal lobe volume in patients with severe symptoms of RTT (Carter et al., 2008). Unlike age-matched healthy normal controls, girls with RTT aged 1 to 14 years demonstrate age-associated (A) increments in the concentrations of myoinositol (mI) and the ratio of mI to creatinine (Cr), and (B) decrements of the ratios of *N*-acetyl aspartic acid to Cr of the white matter of the left frontal region on single-voxel proton magnetic resonance spectroscopy (MRS) (Horská et al., 2009). Diffusion tensor imaging (DTI) fractional anisotropy (FA) of patients with RTT is significantly reduced in the genu and the splenium of the corpus callosum, the external capsule, the anterior cingulate, the internal capsule, the posterior thalamic radiation, and the frontal white matter (Mahmood et al., 2010). The frontal lobes of people with RTT exhibit decrements of blood flow and *N*-acetyl aspartate concentration and increments of glucose metabolism on PET (Naidu et al., 2001).

Abnormalities in the frontal regions of people with RTT correlate with clinical severity of the disabilities of RTT (Carter et al., 2008). Abnormalities in cholinergic neurotransmission from the nucleus basalis of Meynert to the frontal cortex (Johnston et al., 1979) characterize the pathophysiology of RTT. Vesicular acetylcholine binding in the cortex reflects cholinergic axons projecting from the nucleus basalis of Meynert (Johnston et al., 1979), while vesicular acetylcholine binding in the basal ganglia reflects cholinergic interneurons. Forebrain cholinergic neurons are reduced in number in RTT (Wenk and Hauss-Wegrzyniak, 1999). Choline acetyltransferase and vesamicol vesicles, markers of acetylcholine, are diminished in number in the basal ganglia, the hippocampus, the neocortex, and the thalamus of people with RTT (Wenk and Mobley, 1996). In addition, other neurotransmitters are also altered in different brain regions in RTT (Wenk et al., 1991; Wenk, 1997). Choline supplementation of the diets of a murine model revealed deficient forebrain development resulting from abnormalities of acetylcholine neurotransmission, a characteristic that likely plays a role in the pathogenesis and clinical severity of RTT (Berger-Sweeney and Hohmann, 1997; Hohmann and Berger-Sweeney, 1998). Abnormalities of the density and the distribution of the acetylcholine vesicular transporter likely occur in RTT due to decrements in choline acetyltransferase and basal forebrain neurons. The development of a radiotracer to measure this entity represents a major stride to investigate anomalies of acetylcholine transporters in the living human brain. A valuable novel tool to examine the acetylcholine transporter in animals (Sorger et al., 2000) is (+)-*trans*-2-(4-phenylpiperidinyl)cyclohexanol (vesamicol) (Efange, 2000; Efange et al., 2000), a drug to attach to the vesicles that store acetylcholine in vivo (Wenk and Mobley, 1996). [^{3}H]vesamicol binds to the vesicular acetylcholine transporter (ACVT) (Wenk and Mobley, 1996). (−)-*(2R,3R)*-2-hydroxy-3-(4-phenylpiperidino)-5-[^{123}I]iodotetralin, (−)-5-[^{123}I]iodobenzovesamicol ([^{123}I]IBVM], provides the means to estimate the density of acetylcholine vesicular transporters in the living human brain by single photon emission computed tomography (SPECT) (Barret et al., 2008; Jung et al., 1996; Mach et al., 1997; Moriarty, 1994; Zea-Ponce et al., 2005). [^{123}I]IBVM binds to the acetylcholine (ACh) transporter of presynaptic vesicles in the living human brain of healthy adult volunteers (Kuhl et al., 1994, 1996), and in Alzheimer's (Mazère et al., 2008) and Parkinson's diseases (Kuhl et al., 1996). The development of the radiotracer [^{123}I]IBVM (Van Dort et al., 1993) that binds to the ACh transporter of presynaptic vesicles in the living human brain provides a means to map presynaptic terminal acetylcholine densities in individuals with RTT (Emond et al., 2007; Giboureau, et al., 2007).

Therefore, the advent of techniques to visualize the density and distribution of acetylcholine vesicles in the living human brain provides a powerful tool to investigate the neuropathology

and the neurochemistry of RTT. The development of an in vivo procedure to map the integrity of cholinergic neurons in the brains of people with RTT will likely then provide the means to safely and effectively determine the results of pharmacological and other interventions for this disorder. The presynaptic density and distribution of vesicular acetylcholine transporters can be estimated in the living human brain by single-photon emission-computed tomography (SPECT) (Moriarty, 1994) following the intravenous administration of [^{123}I]IBVM (Barret et al., 2008). Binding potentials estimated utilizing reference tissue methods are comparable to those utilizing arterial blood sampling (Barret et al., 2008). Visualization of vesicular acetylcholine transporters in the living human brain by means of SPECT following [^{123}I]IBVM administration also represents a powerful tool to facilitate the diagnoses of other neurodevelopmental disablities, to investigate how alternations in vesicular acetylcholine transporters may reflect clinical variability, to synthesize interventions aimed at the affected vesicular acetylcholine transporters, and to follow changes in vesicular acetylcholine transporters during the course of clinical trials (Zhou et al., 2001).

We hypothesized that the ability to perform the activities of daily living (ADL) is proportional to the density of vesicular acetylcholine transporters in women with RTT.

MATERIALS AND METHODS

Participants

Four participants with RTT with clinical features of the disorder and MeCP2 mutations were recruited from the Neurogenetics Unit of the Kennedy-Krieger Institute and nine healthy normal control volunteer participants were recruited through advertisements placed in Baltimore, Maryland (Table I).

Procedure

The procedure was first performed on the healthy adult volunteer participants to establish the safety, efficacy, and feasibility of the protocol for the participants with RTT.

All participants underwent the construction of a thermoplastic face mask with openings for the eyes, nose, and mouth to position the head for all scans (Figures 1 and 2). Six fiducial markers were placed on the mask to facilitate the positioning of the head in the same location for each scan. Each healthy control participant underwent an MRI of the brain without contrast with a sequence of acquisitions (Brašić et al., 2009, Table II, page 346) for coregistration with the SPECT scan. Since the MRI facility was located in another building, MRI scans were omitted on participants with RTT.

Due to the need for general anesthesia for the participants with RTT for the construction of the facemask as well as for the MRI and SPECT scans, the construction of the facemask and the SPECT scans took place in a single session with general anesthesia lasting approximately 90 to 120 minutes. SPECT scans were performed on a three-headed SPECT Triad/TRIONIX gamma camera with a high resolution collimator.

Conversion of pixel counts from SPECT scans to radioactivity concentrations in MBq/cc—We utilized a phantom scan to measure the correlation of the radioactivity from a sample of the radiotracer with the counts per pixel from a SPECT Triad/TRIONIX gamma camera. At the time of the radiotracer injection into each participant, phantom scans were obtained with the radiotracer on a gamma camera. SPECT acquisitions of the phantom of each participant were reconstructed employing the same filter parameters. First, a SPECT scan was taken of a uniform phantom filled with half a gallon of water containing a

specimen of 37 MBq (1 mCi) of radioactivity [^{123}I]IBVM. A gamma counter then measured the radioactivity counts at the same time in a test tube containing a known volume of the contents of the phantom to yield H, the radioactivity concentration in the phantom, in MBq/cc. SPECT acquisitions of the phantom were obtained for four frames with ten minutes of acquisition per frame. A volume of interest (VOI) was drawn on a representative portion of the SPECT images of ten slices of the phantom. The average pixel concentration value, AvPC, of each phantom VOI, was obtained for ten representative slices of the four frames. For each phantom VOI, the average pixel concentration value per minute, AvPC/min, was calculated by dividing by ten the average pixel value of the phantom VOI for several representative slices of the four frames as follows:

$$\mathrm{AvPC}/10=\mathrm{AvPC}/\mathrm{min} \quad \text{(Equation 1)}$$

The VOIs were drawn on the images of the participant. The pixel counts of the VOIs of the participant, Pa counts, were converted to radioactivity estimates as follows:

$$\mathrm{Pa\,in\,MBq/cc}=\frac{\mathrm{Pa\,counts}}{(\mathrm{AvPC}/\mathrm{min})/(\mathrm{H\,in\,MBq/cc})} \quad \text{(Equation 2)}$$

where Pa is the radioactivity in each VOI of each participant (Equation 2).

Estimation of an index of vesicular acetylcholine transporter density—An arterial line was inserted into the radial artery of six of the healthy control participants to obtain samples of blood to determine radioactivity measurements for time-activity curves and metabolites to verify that the pixels on the images of the gamma camera correlated with the radioactivity of the radiotracer in the plasma following the injection of the radiotracer. A venous line was inserted in the opposite arm for administration of the radiotracer. Three healthy participants and four participants with RTT underwent only the administration of a radiotracer through a venous without arterial blood sampling.

Four participants with RTT and nine healthy adult volunteer control participants underwent SPECT brain scans for sixty (60) minutes at approximately twenty-four (24) hours following the intravenous injection of approximately 333 MBq (9 mCi) [^{123}I]IBVM over 30 seconds (Table I). The participants with RTT underwent general anesthesia for approximately 90 to 120 minutes during a session for the construction of the face mask in approximately 5 minutes and the performance of a 60 minute SPECT acquisition 24 hours after the administration of the [^{123}I]IBVM. The healthy adults did not receive any anesthesia or sedation.

Four separate SPECT acquisitions were obtained for sixty minutes at specific times after the radiotracer injection as follows: 0 to 1 hour, 2.5 to 3.5 hours, 4.5 to 5.5 hours, and 22 to 23 hours. The acquisitions for the first hour included five four-minute frames and four ten-minute frames. The acquisitions at 2.5 to 3.5 hours, 4.5 to 5.5 hours, and 22 to 23 hours, each included six ten-minute acquisitions.

Images were collected using a 128 × 128 matrix. Images were reconstructed on a 64 × 64 matrix with pixel size = 3.56 mm and slice thickness = 3.56 mm. Assuming uniform attenuation equal to the attenuation of water, attenuation correction was applied using a Chang zero-order correction (Chang, 1995; Stelter et al., 2001) with an ellipse was drawn around the skull.

SPECT studies were tilted to obtain a transverse plane at the anterior commissure-posterior commissure (AC-PC) line. The angle of the initial transverse plan to the AC-PC plane was

determined by the MRI co-registered with the SPECT images. The images were corrected for decay and metabolites. Co-registration of MRI and SPECT studies was performed parallel to the AC-PC plane. Polygonal VOIs were drawn on MRI slices to generate time-activity curves on the SPECT slices.

Time-activity curves were obtained for the first six of the healthy control participants who underwent arterial blood sampling. A column-switch high performance liquid chromatography (HPLC) method was employed to analyze the plasma of the arterial blood samples (Hilton et al., 2000). Equilibrium was attained in the striatum and the cerebellum, the reference structure, at approximately 22 to 24 hours after the administration of [^{123}I]IBVM. Figures 3 and 4 demonstrate the time-activity curves at 5.5 and 24 hours respectively for a representative healthy participant, a 21-year-old left-handed man who smokes cigarettes.

The counts generated by the SPECT camera fit the radioactivity measurements of arterial blood sampling with correction for metabolites and decay. Due to technical malfunction of the gamma counter during the initial studies of the 44-year-old healthy control participant, the study was discontinued so many measurements for this participant are missing.

To investigate the tracer kinetic properties of [^{123}I]IBVM in the living human brain during dynamic SPECT scans, we utilized compartmental modeling (Zhou et al., 2001). We employed a 3-compartment 5-parameter model to represent the SPECT kinetics of [^{123}I]IBVM, a reversibly binding radioligand (Zhou et al., 2001). Mathematical modeling of the variable employed for reversibly binding radioligands yielded the results on Table II (Zhou et al., 2001, 2002a,b, 2003). Since the values of k_3 fit the ratios of the corrected radioactivity concentrations in the striatum and the cerebellum, the reference structure, for the four participants with valid measurements (Table II) (Innis et al., 2007; Zhou et al., 2001), we conclude that a modeling method utilizing counts in the pixels of VOIs from the SPECT scans with a reference tissue method are justified.

The maximal uptake of [^{123}I]IBVM occurred in the striata of all participants. There was minimal uptake in the other regions of the brain. We therefore utilized the counts from the SPECT scans to estimate the uptake in the volumes of interest utilizing the counts from the cerebellum as the reference tissue.

The Vesicular Acetylcholine Transporter Binding Site Index (VATBSI), an estimate of the density of vesicular ACh transporters (Kuhl et al., 1994), was estimated in the striatum with the cerebellum as the reference region with minimal uptake. The VATBSI was obtained utilizing the SPECT scans only of all participants (Table I).

Visual representation of [^{123}I]IBVM SPECT images—The outlines of the cortex and selected basal structures (the caudate nucleus, the putamen, and the thalamus, bilaterally) of a standard brain model were aligned in size and orientation to the SPECT radioactivity images in three dimensions (3D). The program for this purpose displayed six images of transverse, coronal, or sagittal views, one view at a time together with outline plots of the studied structures. The program utilized interactive displacement linearly or rotationally or enlargement or shrinkage of the outlined plots as a whole, a half (e.g., left side), or a quarter (e.g., left lower quarter) at selected magnitudes (e.g., 1, 3, and 7 mm for linear displacement) to align the outlined plots to the corresponding outlines given by SPECT images. After the alignment of the cortical outlines, the outlines of the basal structures were aligned separately. The view, displacement type, and displacement magnitude of each trial was stored in files for displacement histories separately for spatial alignments of the cortex and the basal structures. The standard VOIs were transferred to individual SPECT spaces. In the

process, individual grid points (i.e., the centers of voxels) of the SPECT image volumes were displaced in two ways and averaged, being weighted for the distances from the two outline sets. The voxel-cerebellar radioactivity volumes were obtained at each frame around 24 hours post injection (typically three 20 minute frames or two 30 minute frames) and averaged across frames.

VOIs were drawn on the SPECT scans for the striatum, the thalamus, the pons, the occipital cortex, and the cerebellum. The transformed VOIs were applied to the averaged ratio volumes to obtain regional ratios for each frame. The SPECT volumes were averaged across frames taken 24 hours post-injection for individual subjects, after correction for between-scan head movement. Averaged SPECT volumes were aligned to MR volumes in the 8 healthy adult normal control subjects who underwent full SPECT and MR examinations. The MR volumes of the individual subjects were spatially normalized to a standard brain using programs of the SPM99 package (Ashburner and Friston 1997; Ashburner et al., 1997). The SPECT volumes of these subjects were transferred to the standard brain space in the same manner as MR volumes, after transfer to their MR space. The SPECT volumes of the four subjects with RTT without MR volumes were spatially normalized to the same standard brain according to the radioactivity distributions of the eight healthy adult normal control subjects (Haut et al., 2000a, b). The individual SPECT volumes were smoothed using a gaussian kernel (13 mm full-width at half-maximum).

Standard VOIs were applied to spatially normalized SPECT volumes to obtain regional radioactivity at 24 hours post injection. The voxel-cerebellar ratio volumes were generated by dividing voxel radioactivity by the mean cerebellar radioactivity in the individual subjects. The Vesicular Acetylcholine Transporter Binding Site Index (VATSBI) was then calculated as the radioactivity ratio of a specific cerebral structure, i.e., striatum, to the reference structure, the cerebellum, at twenty-four (24) hours post-injection (Table I). The VATSBI represents the density of vesicular acetylcholine transporters of the structure in the numerator (Kuhl et al., 1994).

Assessment of clinical status of participants with RTT—The participants with RTT were carefully evaluated by child neurologists with special competence in Rett syndrome and other neurodevelopmental disabilities in the Neurogenetics Unit of the Kennedy-Krieger Institute. Participants with RTT were rated for ambulation and self-feeding skills and for the severity of respiratory irregularities, rigidity, scoliosis, and seizures (Table III).

RESULTS

Nine healthy adult volunteer participants and four participants with RTT underwent SPECT imaging of the brain 22 to 24 hours after the intravenous administration of approximately 333 MBq (9 mCi) [^{123}I]IBVM. We have summarized the characteristics of the healthy participants (Tables I, II, and IV) and the genetic (Table III) and clinical features (Tables I and III) of the participants with RTT.

Although mean striatal VATSBI is lower in women with RTT (5.2 ± 0.9) than in healthy adults (5.7 ± 1.6) (Table I), a significant difference was not detected utilizing the two-sample Wilcoxon rank-sum (Mann-Whitney) test (StataCorp, 2003). In participants with RTT striatal VATSBI (Table I) and ADL scores (Table III) are linearly associated as follows:

$$ADL=(0.89)^{*}VATSBI+4.5;R^{2}=0.93;p<0.01 \text{ (Brašić et al., 2010a)} \quad \text{(Equation 3)}$$

Figure 5 demonstrates the finding that among women with RTT, VATSBI is (A) directly proportional to the abilities to self feed and to ambulate and (B) inversely proportional to the amount of rigidity on clinical examination. Utilizing the Kruskal-Wallis Test, VATSBI is not significantly associated with any other variables on Table III (StataCorp, 2003).

The Vesicular Acetylcholine Transporter Binding Site Index (VATSBI) ratio volumes were averaged across participants with RTT with SPECT, but not MRI, data (n=4) and healthy adult volunteer normal control participants with full SPECT and MRI data (n=8) (Figure 6) (Haut et al., 2000a, b). The averaged ratio images visually confirm the generalized decrease in vesicular acetylcholine transporter density in women with RTT demonstrated by VOI analysis (Haut et al., 2000a, b).

To explore possibilities for the presence of focal changes in vesicular acetylcholine transporter densities in RTT, we calculated the volume of percent changes in the VATSBI ratio (the normal ratio volume minus the RTT ratio volume divided by the normal ratio volume times 100) (Haut et al., 2000a, b). We selected the clusters of voxels with percent change exceeded 30% and with volumes exceeded 1 mL (Haut et al., 2000a, b). The findings were summarized in Table V and represented in Figure 6 (Haut et al., 2000a, b).

Participants with RTT demonstrated focal areas of decreased vesicular acetylcholine transporters in the striatum in images acquired by SPECT twenty-four hours following the intravenous injection of (−)-5-[^{123}I]iodobenzovesamicol [^{123}I]IBVM (Figure 6) (Table V) (Haut et al., 2000a, b).

Figure 6 demonstrates the VATSBI voxel-to-cerebellar ratio images acquired by SPECT twenty-four hours following the intravenous injection of approximately 333 MBq (9 mCi) [^{123}I]IBVM spatially normalized and averaged across 8 normal healthy adult control participants (upper panels) and across 4 participants with RTT (lower panels). The ratio, an estimate of acetylcholine transporter density in presynaptic vesicles, was reduced in SPECT images after the injection of [^{123}I]IBVM in people with RTT in the vermis (left lower panel), the bilateral precentral cortices (left lower panel), the striatum (middle lower panel), and middle cingulate (right middle panel) (Figure 6) (Haut et al., 2000a, b).

Due to the small sample size (4 experimental participants and 9 control participants) descriptive, not analytical, statistics were used to assess the results in this preliminary study (Brašić et al., 2003b). Vesicular acetylcholine transporter density was reduced in some subjects with RTT. Reductions in the VATSBI in the putamen are associated with rigidity and impairments in the performance of activities of daily living in some women with RTT (Bibat et al., 2003, 2004; Brašić et al., 2003a; Dogan et al., 2003).

The participant with RTT with the highest VATSBI (Table I) and the best performance of ADL skills (Table III) exhibited skewed X-inactivation (Table III) (Bibat et al., 2003, 2004) suggesting that skewed X-inactivation may modify the symptoms of RTT.

DISCUSSION

SPECT brain imaging 22 to 24 hours after the intravenous administration of [^{123}I]IBVM was obtained on nine healthy adult volunteer participants and four participants with RTT and mutations in the MECP2 gene. An index to estimate vesicular ACh transporters was significantly correlated with the abilities to perform certain activities of daily living (ADL) in the women with RTT. This correlation of the ability to perform key activities of daily living (ADL) to a density index of vesicular ACh transporters in the striata of women with RTT suggests that [^{123}I]IBVM may be a promising tool to characterize the pathophysiological mechanisms of RTT.

The higher resolution and the decreased study duration of PET are definite reasons to consider planning future studies with [^{18}F]fluoroethoxybenzovesamicol, ((−)-[^{18}F]FEOBV), (−)-*(2R,3R)-trans*-2-hydroxy-3-(4-phenylpiperidino)-5-(2-[^{18}F]fluoroethoxy)-1,2,3,4-tetralin (Mulholland et al., 1998), [^{18}F] (+)-4-fluorobenzyltrozamicol ((+)-[^{18}F]FBT) (Voytko et al., 2001), and other PET radioligands for the vesicular ACh transporters.

We showed that [^{123}I]IBVM SPECT may be a safe, effective technique to estimate the integrity of the acetylcholinergic system in RTT (Brašić et al., 2003a). The VATSBI appears to be an appropriate tool to estimate the binding of vesicular acetylcholine transporters in the living human brain. Our preliminary findings supports the hypothesis that impaired ability to perform the activities of daily living may be associated with deficits in vesicular acetylcholine transporter binding in the striatum in RTT (Brašić et al., 2010a) needs validation in a larger study. Therapeutic interventions for RTT may be monitored by serial performance of [^{123}I]IBVM SPECT before, during, and after clinical trials. Further research is needed to clarify the biological basis for the pathognomonic abnormalities in movement and neurochemistry in RTT (Brasić, 1999) including demographic data about study populations to identify racial and ethnic variations (Brašić, 2003, 2004).

Since potential treatments include choline acetyltransferase, the enzyme that synthesizes acetylcholine, future studies may benefit from measurement of levels of choline acetyltransferase to confirm the reductions of choline acetyltransferase observed in a subset of people with RTT (Bibat et al., 2003, 2004).

The participants with RTT underwent SPECT scans under general anesthesia, which possibly could introduce alterations in the binding of [^{123}I]IBVM throughout the brain. An optimal experimental design includes the utilization of exactly the same protocol for all participants, both experimental and control participants. However, the participants with RTT are unable to hold still for the study procedures or understand the protocol. During attempts to manually stabilize the head for the construction of a facemask (Figures 1 and 2), the participants with RTT had movement artifacts requiring general anesthesia to obtain facemasks and scans of quality for the analysis. The healthy participants did not need to be subjected to any unnecessary risks of general anesthesia. Hopefully techniques to scan participants with RTT without anesthesia may become available in the future.

The occurrence of reductions in vesicular acetylcholine transporters and high-affinity $\alpha 4\beta 2$ neuronal nicotinic acetylcholine receptors (nAChRs) in the brains of rats treated with the cholinergic immunolesioning agent 192 IgG-saporin (SAP) (Quinlivan et al., 2007) suggests that reductions in high-affinity $\alpha 4\beta 2$ nAChRs may occur along with reductions in vesicular acetylcholine transporters in people with RTT. Multimodal imaging of the density and the distribution of vesicular acetylcholine transporters and high-affinity $\alpha 4\beta 2$ AChRs (Brašić et al., 2010a,b) in people with RTT offers the promise of a potential useful procedure to characterize clinical severity of RTT and to provide rational therapies for the syndrome, and represents a possibly useful tool to quantify the cholinergic system in other disorders.

Additionally future studies in different geographical locations with larger samples of participants may be useful when researching the therapeutic efficacy or the clinical severity of the disease for purposes of intervention.

Ethical aspects are an important consideration as participants with RTT lack the cognitive capacity to understand proposed research studies (Brašić et al., 2002, Chun et al., 2002). Although participants with RTT are unable to provide informed consent to take part in research to characterize the alterations in the living human brain, they are necessary components of the process to develop effective remedies for the syndrome. We seek to share with those who may benefit the findings of this first investigation to correlate the abilities to

perform certain activities of daily living with the density of the vesicular acetylcholine transporter in the living brains of women with RTT. Investigations to characterize the neurochemical dysfunction in the living brains of people with RTT are the crucial first steps in the process to develop effective interventions to treat the abnormalities. The risks of general anesthesia in women with RTT are justified to advance the knowledge of the condition for the future benefit of others with RTT and related neurodevelopmental disabilities. Although there is no direct benefit to the participants themselves, there is potentially great benefit to future generations of victims with RTT and related conditions. Legislation to prohibit research without therapeutic components prevents the pilot studies crucial to develop rational therapies for neurodevelopmental disabilities. We encourage others to develop the current findings to design effective therapies for RTT and related disorders.

Acknowledgments

This research was sponsored by the National Alliance for Research on Schizophrenia and Depression (NARSAD) (JRB), the Essel Foundation (JRB), and the National Institutes of Health (NIH) by Public Health Service Grant HD24448 (SN), DA09482 (DFW), and NCRR M01RR00052 (Clinical Research Unit). Dr. Brašić is a member of the Medical Advisory Board of the Tourette Syndrome Association of Greater Washington, Silver Spring, Maryland.

References

Amir RE, Van den Veyver IB, Schultz R, Malicki DM, Tran CQ, Dahle EJ, Philippi A, Timar L, Percy AK, Motil KJ, Lichtarge O, Smith EO, Glaze DG, Zoghbi HY. Influence of mutation type and X chromosome inactivation on Rett syndrome phenotypes. Ann Neurol. 2000; 47:670–679. [PubMed: 10805343]

Amir RE, Van den Veyver IB, Wan M, Tran CQ, Francke U, Zoghbi HY. Rett syndrome is caused by mutations in X-linked MECP2, encoding methyl-CpG-binding protein 2. Nat Genet. 1999; 23:185–188. [letter]. [PubMed: 10508514]

Amir RE, Zoghbi HY. Rett syndrome: methyl-CpG-binding protein 2 mutations and phenotype-genotype correlations. Am J Med Genet. 2000; 97(2):147–152. [PubMed: 11180222]

Armstrong DD. Neuropathology of Rett syndrome. J Child Neurol. 2005; 20:747–753. [PubMed: 16225830]

Armstrong DD. Neuropathology of Rett syndrome. Ment Retard Dev Disabil Res Rev. 2002; 8:72–76. [PubMed: 12112730]

Armstrong DD. Rett syndrome neuropathology review 2000. Brain Devel. 2001; 23(Suppl 1):S72–S76. [PubMed: 11738845]

Ashburner J, Friston K. Multimodal image coregistration and partitioning - a unified framework. NeuroImage. 1997; 6:209–217. [PubMed: 9344825]

Ashburner J, Neelin P, Collins DL, Evans A, Friston K. Incorporating prior knowledge into jmage registration. NeuroImage. 1997; 6:344–352. [PubMed: 9417976]

Barret O, Mazère J, Seibyl J, Allard M. Comparison of noninvasive quantification methods of in vivo vesicular acetylcholine transporter using [^{123}I]-IBVM SPECT imaging. J Cereb Blood Flow Metab. 2008; 28:1624–1634. [PubMed: 18506194]

Bebbington A, Anderson A, Ravine D, Fyfe S, Pineda M, de Klerk N, Ben-Zeev B, Yatawara N, Percy A, Kaufmann WE, Leonard H. Investigating genotype-phenotype relationships in Rett syndrome using an international data set. Neurology. 2008; 70(11):868–875. [PubMed: 18332345]

Bebbington A, Percy A, Christodoulou J, Ravine D, Ho G, Jacoby P, Anderson A, Pineda M, Ben Zeev B, Bahi-Buisson N, Smeets E, Leonard H. Updating the profile of C-terminal MECP2 deletions in Rett syndrome. J Med Genet. 2010; 47:242–248. [PubMed: 19914908]

Berger-Sweeney J, Hohmann CF. Behavioral consequences of abnormal cortical development: insights into developmental disabilities. Behav Brain Res. 1997; 86:121–142. [PubMed: 9134147]

Bibat GM, Brasic JR, Dogan AS, Kuwabara H, Maini A, Maris MA, Hoffman EP, Blue ME, Johnston MV, Wong DF, Naidu S. Determination of presynaptic acetylcholine terminal densities and its clinical correlation in Rett's syndrome. Ann Neurol. 2003; 54(suppl 7):S118. [abstract].

Bibat GM, Brasic JR, Dogan AS, Kuwabara H, Maini A, Maris MA, Naidu S, Wong DF. Reduced acetylcholine vesicular transport in adults with Rett syndrome: clinical correlation and therapeutic implications. Neurology. 2004; 62(suppl 5):A28. [abstract].

Brasić JR. Movements in autistic disorder. Med Hypotheses. 1999; 53(1):48–49. [PubMed: 10499825]

Brašić JR. Documentation of demographic data. Psychol Rep. 2003; 93:151–152. [PubMed: 14563042]

Brašić JR. Documentation of ethnicity. Psychol Rep. 2004; 95 (3):859–861. [PubMed: 15666919]

Brašić JR, Bibat G, Hiroto K, Kumar A, Zhou Y, Hilton JD, Yablonski MB, Dogan AS. Correlations of the ability to perform the activities of daily living (ADL) to a density index of acetylcholine (ACh) vesicular transporters in the striata of women with Rett syndrome (RTT). J Nucl Med. 2010a; 51(5):830–831. [abstract].

Brasic, JR.; Bradford, L.; Kalaff, A.; Sims, LP.; Alexander, M.; Maini, A.; Dogan, AS.; Chun, TT.; Bibat, G.; Naidu, S.; Coenraads, M.; Wong, DF. Improving the quality of research with human subjects with Rett syndrome. 3rd Annual Rett Syndrome Symposium; Baltimore, Maryland. June 17–19, 2002; Cincinnati, Ohio: Rett Syndrome Research Foundation; 2002. p. 29(www.rsrf.org) [abstract]

Brasic JR, Cascella N, Hussain B, Bisuna B, Kumar A, Raymont V, Guevara MR, Horti A, Wong DF. PET experience with (2-[^{18}F]fluoro-3-(2(S)-azetidinylmethoxy)pyridine (2-[^{18}F]FA) in the living human brain of smokers and nonsmokers. J Nucl Med. 2010b; 51(supplement 2):388P. [abstract].

Brašić, JR.; Dogan, AS.; Kuwabara, H.; Maini, A.; Bibat, G.; Naidu, S.; Maris, MA.; Wong, DF. Deficient presynaptic acetylcholine terminal densities in the brains of adults with Rett syndrome who demonstrate impaired performance of the activities of daily living. 4th Annual Rett Syndrome Symposium; Baltimore, Maryland. June 23–25, 2003; Rett Syndrome Research Foundation; 2003a. p. 29(www.rsrf.org)[abstract]

Brašić, JR.; Rohde, CA.; Maris, MA.; Wong, DF. Sample size determination for studies of Rett syndrome and other rare conditions. 4th Annual Rett Syndrome Symposium; Baltimore, Maryland. June 23–25, 2003; Rett Syndrome Research Foundation; 2003b. p. 46(www.rsrf.org)[abstract]

Brašić JR, Zhou Y, Musachio JL, Hilton J, Fan H, Crabb A, Endres CJ, Reinhardt MJ, Dogan AS, Alexander M, Rousset O, Maris MA, Galecki J, Nandi A, Wong DF. Single photon emission computed tomography experience with (*S*)-5-[^{123}I]iodo-3-(2-azetidinylmethoxy)pyridine in the living human brain of smokers and nonsmokers. Synapse. 2009; 63(4):339–358. [PubMed: 19140167]

Carter JC, Lanham DC, Pham D, Bibat G, Naidu S, Kaufmann WE. Selective cerebral volume reduction in Rett syndrome: a multiple-approach MR imaging study. AJNR Am J Neuroradiol. 2008; 29:436–441. [PubMed: 18065507]

Chang S-C. The method of space-time conservation element and solution element--A new approach for solving the Navier-Stokes and Euler equations. J Comput Phys. 1995; 119(2):295–324.

Chun, TT.; Brašić, JR.; Morgan, RH. Is research on human being with Rett syndrome ethical?. 3rd Annual Rett Syndrome Symposium; Baltimore, Maryland. June 17–19, 2002; Rett Syndrome Research Foundation; 2002. p. 30(www.rsrf.org)[abstract]

Dogan AS, Brasic JR, Kuwabara H, Maini A, Bibat G, Naidu S, Wong DF. Deficiencies of striatal vesicular acetylcholine transporter binding and activities of daily living in Rett disorder. J Nuc Med. 2003; 44(5 suppl):15P. [abstract].

Efange SMN. In vivo imaging of the vesicular acetylcholine transporter and the vesicular monoamine transporter. FASEB J. 2000; 14:2401–2413. [PubMed: 11099458]

Efange SMN, von Hohenberg K, Khare AB, Tu Z, Mach RH, Parsons SM. Synthesis and biological characterization of stable and radioiodinated (+/−)-trans-2-hydroxy-3-P[4-(3-iodophenyl)piperidyl]-1,2,3,4-tetrahydronaphthalene (3′-IBVM). Nucl Med Biol. 2000; 27:749–755. [PubMed: 11150707]

Emond P, Mavel S, Zea-Ponce Y, Kassiou M, Garreau L, Bodard S, Drossard M-L, Chalon S, Guilloteau D. (E)-[^{125}I]-5-AOIBV: a SPECT radioligand for the vesicular acetylcholine transporter. Nucl Med Biol. 2007; 34:967–971. [PubMed: 17998100]

Giboureau N, Emond P, Fulton RR, Henderson DJ, Chalon S, Garreau L, Roselt P, Eberl S, Mavel S, Bodard S, Fulham MJ, Guilloteau D, Kassiou M. Ex vivo and in vivo evaluation of *(2R,3R)*-5-[^{18}F]-fluoroethoxy- and fluoropropoxy-benzovesamicol, as PET radioligands for the vesicular acetylcholine transporter. Synapse. 2007; 61:962–970. [PubMed: 17787004]

Hagberg B, Aicardi J, Dias K, Ramos O. A progressive syndrome of autism, dementia, ataxia, and loss of purposeful hand use in girls: Rett's syndrome: report of 35 cases. Ann Neurol. 1983; 14:471–479. [PubMed: 6638958]

Haut MW, Kuwabara H, Leach S, Arias RG. Neural activation during performance of number-letter sequencing. Appl Neuropsychol. 2000a; 7(4):237–242. [PubMed: 11296686]

Haut MW, Kuwabara H, Leach S, Ty Callahan T. Age-related changes in neural activation during working memory performance. Neuropsychol Dev Cogn B Aging Neuropsychol Cogn. 2000b; 7 (2):119– 129.

Hilton J, Yokoi F, Dannals RF, Ravert HT, Szabo Z, Wong DF. Column-switching HPLC for the analysis of plasma in PET imaging studies. Nucl Med Biol. 2000; 27:627–630. [PubMed: 11056380]

Hoffbuhr K, Devaney JM, LaFleur B, Sirianni N, Scacheri C, Giron J, Schuette J, Innis J, Marino M, Philippart M, Narayanan V, Umansky R, Kronn D, Hoffman EP, Naidu S. MeCP2 mutations in children with and without the phenotype of Rett syndrome. Neurology. 2001; 56:1486–1495. [PubMed: 11402105]

Hoffbuhr KC, Moses LM, Jerdonek MA, Naidu S, Hoffman EP. Associations between MECP2 mutations, X-chromosome inactivation, and phenotype. Ment Retard Devel Disabil Res Rev. 2002; 8:99–105. [PubMed: 12112735]

Hohmann CF, Berger-Sweeney J. Cholinergic regulation of cortical development and plasticity: new twists to an old story. Perspect Dev Neurobiol. 1998; 5:401–425. [PubMed: 10533528]

Horská A, Farage L, Bibat G, Nagae LM, Kaufmann WE, Barker PB, Naidu S. Brain metabolism in Rett syndrome: age, clinical, and genotype correlations. Ann Neurol. 2009; 65:90–97. [PubMed: 19194883]

Innis RB, Cunningham VJ, Delforge J, Fujita M, Gjedde A, Gunn RN, Holden J, Houle S, Huang SC, Ichise M, Iida H, Ito H, Kimura Y, Koeppe RA, Knudsen GM, Knuuti J, Lammertsma AA, Laruelle M, Logan J, Maguire RP, Mintun MA, Morris ED, Parsey R, Price JC, Slifstein M, Sossi V, Suhara T, Votaw JR, Wong DF, Carson RE. Consensus nomenclature for in vivo imaging of reversibly binding radioligands. J Cereb Blood Flow Metab. 2007; 27:1533–1539. [PubMed: 17519979]

Johnston MV, Jeon O-H, Pevsner J, Blue ME, Naidu SB. Neurobiology of Rett syndrome: a genetic disorder of synapse development. Brain Dev. 2001; 23 (suppl 1):S206–S213. [PubMed: 11738874]

Johnston MV, McKinney M, Coyle JT. Evidence for a cholinergic projection to neocortex from neurons in basal forebrain. Proc Natl Acad Sci U S A. 1979; 76:5392–5396. [PubMed: 388436]

Jung Y-W, Frey KA, Mulholland GK, del Rosario R, Sherman PS, Raffel DM, Van Dort ME, Kuhl DE, Gildersleeve DL, Wieland DM. Vesamicol receptor mapping of brain cholinergic neurons with radioiodine-labeled positional isomers of benzovesamicol. J Med Chem. 1996; 39:3331–3342. [PubMed: 8765517]

Kuhl DE, Koeppe RA, Fessler JA, Minoshima S, Ackermann RJ, Carey JE, Gildersleeve DL, Frey KA, Wieland DM. In vivo mapping of cholinergic neurons in the human brain using SPECT and IBVM. J Nucl Med. 1994; 35:405–410. [PubMed: 8113884]

Kuhl DE, Minoshima S, Fessler JA, Frey KA, Foster NL, Ficaro EP, Wieland DM, Koeppe RA. In vivo mapping of cholinergic terminals in normal aging, Alzheimer's disease, and Parkinson's disease. Ann Neurol. 1996; 40:399–410. [PubMed: 8797529]

Leonard, H.; Colvin, L.; Fyfe, S.; Christodoulou, J.; Raffaele, L.; Leonard, S.; Schiavello, T.; Ellaway, C.; Davis, M.; De Kierk, N. Now that the gene has been found: describing the phenotype in Rett syndrome using a national database. 3rd Annual Rett Syndrome Symposium; Baltimore,

Maryland. June 17–19, 2002; Rett Syndrome Research Foundation; 2002. p. 41-42.(www.rsrf.org) [abstract]

Mach RH, Voytko ML, Ehrenkaufer RLE, Nader MA, Tobin JR, Efange SMN, Parsons SM, Gage HD, Smith CR, Morton TE. Imaging of cholinergic terminals using the radiotracer [^{18}F](+)-4-fluorobenzyltrozamicol: in vitro binding studies and positron emission tomography studies in nonhuman primates. Synapse. 1997; 25:368–380. [PubMed: 9097396]

Mahmood A, Bibat G, Zhan A-L, Izbudak I, Farage L, Horska A, Mori S, Naidu S. White matter impairment in Rett Syndrome: diffusion tensor imaging study with clinical Correlations. AJNR Am J Neuroradiol. 2010; 31:295–299. [PubMed: 19833797]

Mazère J, Prunier C, Barret O, Guyot M, Hommet C, Guilloteau D, Dartigues JF, Auriacombe S, Fabrigoule C, Allard M. In vivo SPECT imaging of vesicular acetylcholine transporter using [123I]-IBVM in early Alzheimer's disease. NeuroImage. 2008; 40:280–288. [PubMed: 18191587]

Moriarty J. The value of single photon emission tomography in psychopharmacology. Hum Psychopharmacol. 1994; 9:357–364.

Mulholland GK, Wieland DM, Kilbourn MR, Frey KA, Sherman PS, Carey JE, Kuhl DE. [^{18}F]fluoroethoxy-benzovesamicol, a PET radiotracer for the vesicular acetylcholine transporter and cholinergic synapses. Synapse. 1998; 30:263–274. [PubMed: 9776130]

Naidu S. Rett syndrome: from discovery to current interest. J Child Neurol. 2003; 18:661. [editorial]. [PubMed: 14649545]

Naidu S. Rett syndrome: a disorder affecting early brain growth. Ann Neurol. 1997a; 42:3–10. [PubMed: 9225679]

Naidu SB. Rett syndrome. Indian J Pediatr. 1997b; 64:651–659. [PubMed: 10771898]

Naidu S, Bibat G, Kratz L, Kelley RI, Pevsner J, Hoffman E, Cuffari C, Rohde C, Blue ME, Johnston MV. Clinical variability in Rett syndrome. J Child Neurol. 2003; 18:662–668. [PubMed: 14649546]

Naidu S, Kaufmann WE, Abrams MT, Pearlson GD, Lanham DC, Fredericksen KA, Barker PB, Horska A, Golay X, Mori S, Wong DF, Yablonski M, Moser HW, Johnston MV. Neuroimaging studies in Rett syndrome. Brain Dev. 2001; 23(suppl 1):S62–S71. [PubMed: 11738844]

Neul JL, Fang P, Barrish J, Lane J, Caeg EB, Smith EO, Zoghbi H, Percy A, Glaze DG. Specific mutations in methyl-CpG-binding protein 2 confer different severity in Rett syndrome. Neurology. 2008; 70(16):1313–1321. [PubMed: 18337588]

Percy AK, Lane JB, Childers J, Skinner S, Annese F, Barrish J, Caeg E, Glaze DG, MacLeod P. Rett syndrome: North American database. J Child Neurol. 2007; 22:1338–1241. [PubMed: 18174548]

Online Mendelian Inheritance in Man (OMIM). http://www.ncbi.nlm.nih.gov/Omim. (verified September 13, 2011)

Quinlivan M, Chalon S, Vergote J, Henderson J, Katsifis A, Kassiou M, Guilloteau D. Decreased vesicular acetylcholine transporter and α4β2 nicotinic receptor density in the rat brain following 192 IgG-saporin immunolesioning. Neurosci Lett. 2007; 415:97–101. [PubMed: 17339079]

Rett A. Ueber ein eigenartiges hirnatrophisches Syndrom bei Hyperammoniimie in Kindesalter [On a unusual brain atrophy syndrome in hyperammonemia in childhood]. Wien Med Wochenschr. 1966; 116(37):723–726. [PubMed: 5300597]

Ronnett GV, Leopold D, Cai X, Hoffbuhr KC, Moses L, Hoffman EP, Naidu S. Olfactory biopsies demonstrate a defect in neuronal development in Rett's syndrome. Ann Neurol. 2003; 54:206–218. [PubMed: 12891673]

Sirianni N, Naidu S, Pereira J, Pillotto RF, Hoffman EP. Rett Syndrome: confirmation of X-linked dominant inheritance, and localization of the gene to Xq28. Am J Hum Genet. 1998; 63:1552–1558. [letter]. [PubMed: 9792883]

Sorger D, Schliebs R, Kämpfer I, Rossner S, Heinicke J, Dannenberg C, Georgi P. In vivo [^{125}I]-iodobenzovesamicol binding reflects cortical cholinergic deficiency induced by specific immunolesion of rat basal forebrain cholinergic system. Nucl Med Biol. 2000; 27:23–31. [PubMed: 10755642]

StataCorp. Stata Statistical Software: Release 8.0. College Station, TX: Stata Corporation; 2003.

Stelter P, Junik R, Krzyminiewski R, Gembicki M, Sowiński J. Semiquantitative analysis of SPECT images using ^{99}Tc^{m}-HMPAO in the treatment of brain perfusion after the attenuation correction

by the Chang method and the application of the Butterworth filter. Nucl Med Commun. 2001; 22(8):857–865. [PubMed: 11473204]

Van Dort ME, Jung YW, Gildersleeve DL, Hagen CA, Kuhl DE, Wieland DM. Synthesis of the ^{123}I- and ^{125}I-labeled cholinergic nerve marker (−)-5-iodobenzovesamicol. Nucl Med Biol. 1993; 20(8):929–937. [PubMed: 8298572]

Voytko ML, Mach RH, Gage HD, Ehrenkaufer RLE, Efange SMN, Tobin JR. Cholinergic activity of aged Rhesus monkeys revealed by positron emission tomography. Synapse. 2001; 39:95–100. [PubMed: 11071714]

Wan M, Lee SS, Zhang X, Houwink-Manville I, Song HR, Amir RE, Budden S, Naidu S, Pereira JL, Lo IF, Zoghbi HY, Schanen NC, Francke U. Rett syndrome and beyond: recurrent spontaneous and familial MECP2 mutations at CpG hotspots. Am J Hum Genet. 1999; 65:1520–1529. [PubMed: 10577905]

Wenk GL. Rett syndrome: neurobiological changes underlying specific symptoms. Prog Neurobiol. 1997; 51(4):383–391. [PubMed: 9106898]

Wenk GL, Hauss-Wegrzyniak B. Altered cholinergic function in the basal forebrain of girls with Rett syndrome. Neuropediatrics. 1999; 30:125–129. [PubMed: 10480206]

Wenk GL, Mobley SL. Choline acetyltransferase activity and vesamicol binding in Rett syndrome and in rats with nucleus basalis lesions. Neuroscience. 1996; 73:79–84. [PubMed: 8783231]

Wenk GL, Naidu S, Casanova MF, Kitt CA, Moser H. Altered neurochemical markers in Rett's syndrome. Neurology. 1991; 41:1753–1756. [PubMed: 1658685]

Zea-Ponce Y, Mavel S, Assaad T, Kruse SE, Parsons SM, Emond P, Chalon S, Giboureau N, Kassiou M, Guilloteau D. Synthesis and in vitro evaluation of new benzovesamicol analogues as potential imaging probes for the vesicular acetylcholine transporter. Bioorg Med Chem. 2005; 13:745–753. [PubMed: 15653342]

Zhou, Y.; Bražić, JR.; Fan, H.; Maini, A.; Wong, DF. Kinetic analysis and parametric imaging of [^{123}I](*S*)-5-iodo-3-(2-azetidinylmethoxy)pyridine (5IA) for subjects with Rett syndrome. 3rd Annual Rett Syndrome Symposium; Baltimore, Maryland. June 17–19, 2002; Rett Syndrome Research Foundation; 2002a. p. 31(www.rsrf.org)[abstract]

Zhou, Y.; Brasic, JR.; Musachio, JL.; Zukin, SR.; Kuwabara, H.; Crabb, AH.; Endres, CJ.; Hilton, J.; Fan, H.; Wong, DF. Human [^{123}I]5-I-A-85380 dynamic SPECT studies in normals: kinetic analysis and parametric imaging. Nuclear Science Symposium Conference Record, 2001 IEEE (Institute of Electrical and Electronics Engineers); 2001. p. 1335-1340.

Zhou Y, Endres CJ, Brašić JR, Huang S-C, Wong DF. Linear regression with spatial constraint to generate parametric images of ligand-receptor dynamic PET studies with a simplified reference tissue model. NeuroImage. 2003; 18:975–989. [PubMed: 12725772]

Zhou, Y.; Endres, CJ.; Dogan, AS.; Brasic, JR.; Wong, DF.; Huang, S-C. A new linear parametric imaging algorithm derived from a simplified reference tissue model for ligand-receptor dynamic PET studies. In: Senda, M.; Kimura, Y.; Herscovitch, P., editors. Brain Imaging Using PET. Amsterdam: Academic Press; 2002b. p. 33-39.

Zoghbi HY. Postnatal neurodevelopmental disorders: meeting at the synapse? Science. 2003; 302:826–830. [PubMed: 14593168]

Fig. 1.
Superior view of thermoplastic facemask worn by all subjects in both magnetic resonance imaging (MRI) and single-photon emission-computed tomography (SPECT) to stabilize head in the desired position. Photograph provided courtesy of Dr. Wichana Chamroonrat, Division of Nuclear Medicine, The Russell H. Morgan Department of Radiology and Radiological Science, School of Medicine, The Johns Hopkins University School of Medicine, Baltimore, Maryland.

Fig. 2.

Anterior view of thermoplastic facemask worn by all subjects in both magnetic resonance imaging (MRI) and single-photon emission-computed tomography (SPECT) to stabilize head in the desired position. Photograph provided courtesy of Dr. Wichana Chamroonrat, Division of Nuclear Medicine, The Russell H. Morgan Department of Radiology and Radiological Science, School of Medicine, The Johns Hopkins University School of Medicine, Baltimore, Maryland.

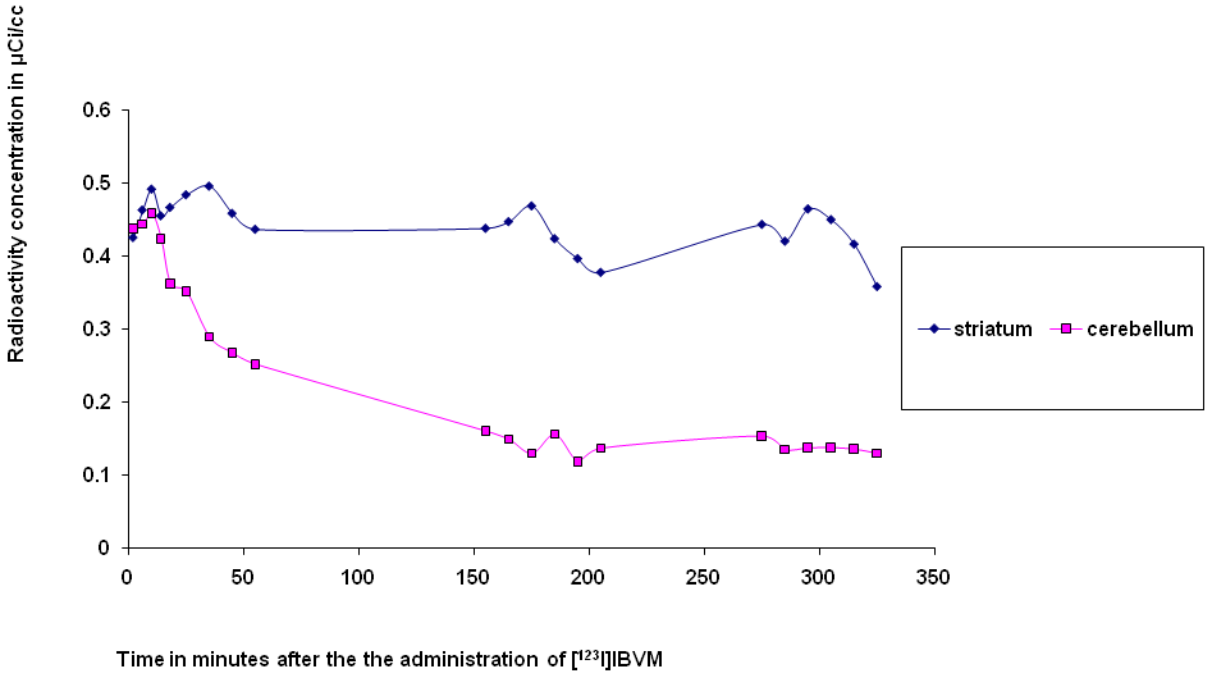

Fig. 3.

Radioactivity concentration in the indicated volumes of interest (VOIs) for 5.5 hours after the intravenous administration of approximately 333 MBq (9 mCi) (−)-5-[^{123}I]iodobenzovesamicol ([^{123}I]IBVM) to a healthy left-handed 21-year-old man who smokes cigarettes.

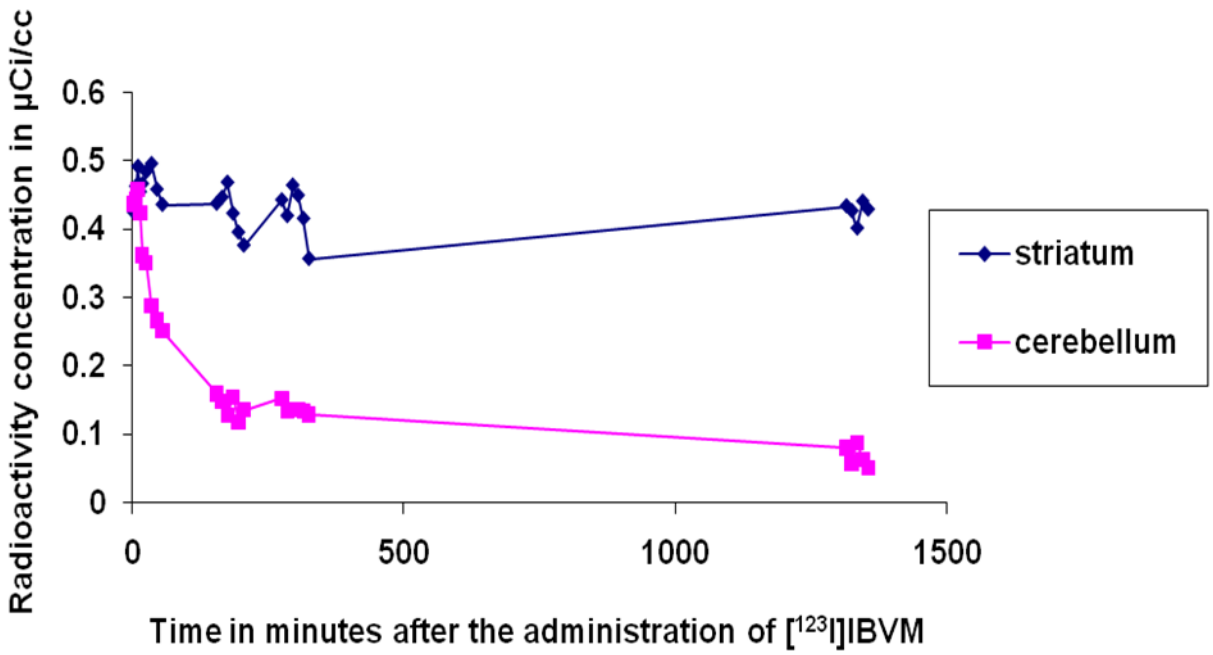

Fig. 4.

Radioactivity concentration in the indicated volumes of interest (VOIs) for 24 hours after the intravenous administration of approximately 333 MBq (9 mCi) (−)-5-[^{123}I]iodobenzovesamicol ([^{123I}]IBVM) to a healthy left-handed 21-year-old man who smokes cigarettes.

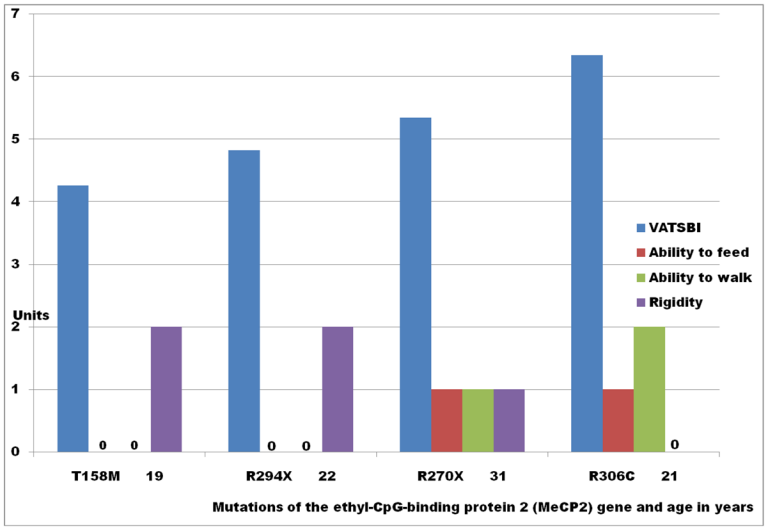

Fig. 5.

Vesicular Striatal Vesicular Acetylcholine Transporter Binding Site Index (VATBSI) scores and clinical characteristics of women with Rett syndrome (RTT) with mutations of the methyl-CpG-binding protein 2 (MeCP2) gene. The specific mutations of the MeCP2 gene and the age in years are presented on the abscissa. The units of the VATSBI and the clinical scores of each person are presented on the ordinate. Participants were given a score of 1 if they can feed themselves and 0 if they cannot feed themselves. Participants were given a score of 2 if they can walk without assistance, 1 if they can walk with assistance, and 0 if they cannot walk. Participants were given a score of 2 if they exhibit marked rigidity, 1 if they exhibit mild rigidity, and 0 if they exhibit no rigidity.

VATBSI scores are directly proportional to the ability to feed self and to the ability to ambulate. VATBSI scores are inversely proportional to the amount of rigidity. The 21-year-old participant with the R306C mutation, the only participant with skewed X-inactivation, exhibited the highest VATSBI scores and the abilities to feed self and to walk without assistance.

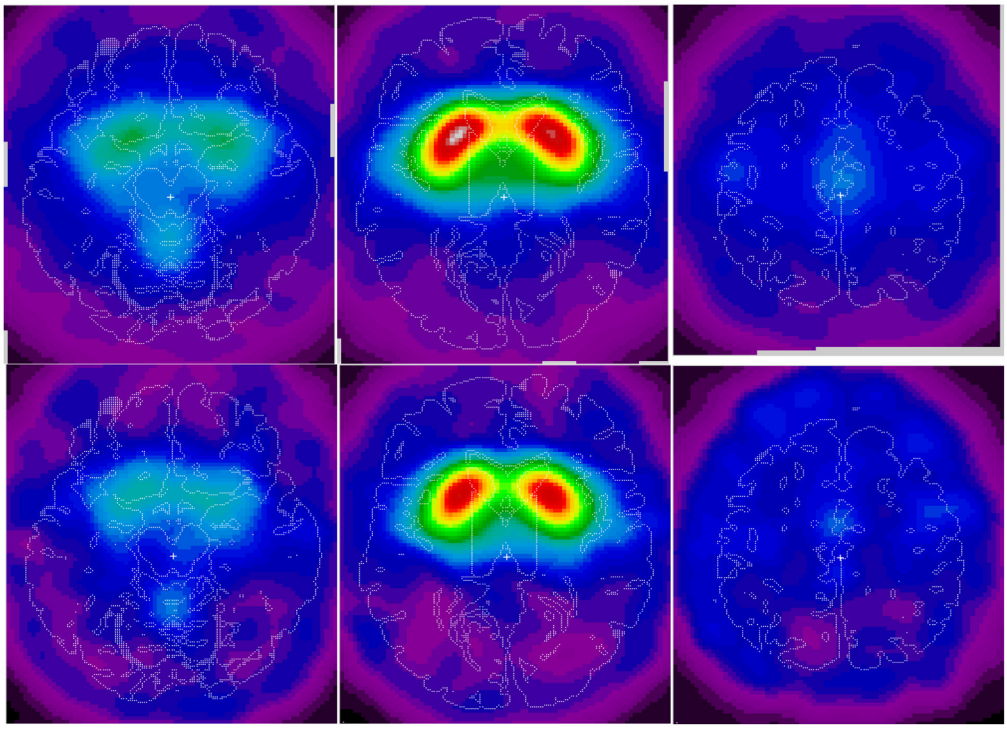

Fig. 6.

Upper panels: Voxel-to-cerebellar ratio images acquired by SPECT 24 h following the intravenous injection of approximately 333 MBq (9 mCi) (2)-5-[^{123}I]iodobenzovesamicol ([^{123}I]IBVM), spatially normalized and averaged across eight healthy volunteer normal control adult participants (upper panels). The left of each image corresponds to the left of the brain. The right of each image corresponds to the right of the brain. The top of each image corresponds to the anterior aspect (front) of the brain. The bottom of each image corresponds to the posterior aspect (back) of the brain. T1-weighted MRI was obtained on the brains of all subjects. The radioactivity from [^{123}I]IBVM during SPECT is obtained for the striatum, the thalamus, the pons, the occipital cerebral cortex, and the cerebellum using VOIs defined on the MRI and transferred to the SPECT image space. The panels represent transverse slices of the brain at the level of the cerebellum (left), striatum (middle), and cingulate gyrus (right) (Haut et al., 2000a,b).

Lower panels: Schematic representations of areas of decreased voxel-cerebellar ratios of images of the brain generated by single-photon emission-computed tomography (SPECT) following the intravenous administration of approximately 333 MBq (9 mCi) (2)-5-[^{123}I]iodobenzovesamicol ([^{123}I]IBVM) spatially normalized and averaged across four participants with RTT. MRIs were not obtained for any participant with RTT. The left of each image corresponds to the left of the brain. The right of each image corresponds to the right of the brain. The top of each image corresponds to the anterior aspect (front) of the brain. The bottom of each image corresponds to the posterior aspect (back) of the brain. Clusters of voxels were identified for subjects with RTT with volumes exceeding 1 mL with voxel-cerebellar ratios reduced by at least 30% in subjects with RTT. Although the limited number of subjects precluded statistical inference, the findings suggested the potential presence of focal areas of decreased vesicular acetylcholine transporters in RTT. The panels represent transverse slices of the brain at the level of the cerebellum (left lower panel), striatum (middle lower panel), and cingulate gyrus (right lower panel). Presented in the figure are the decrements in uptake in the vermis (left lower panel), the striatum (middle

lower panel), and in bilateral precentral cortices (left lower panel) and middle cingulate (right lower panel) (Haut et al., 2000a,b).

TABLE I

Characteristics of participants who received single-photon emission-computed tomography (SPECT) of the brain for sixty (60) minutes, twenty-four (24) hours following the intravenous injection of approximately 333 MBq (9 mCi) (−)-5-[^{123}I]iodobenzovesamicol ([^{123}I]IBVM)

Diagnosis	Age in years	Sex	Ethnicity	Arterial blood sampling	[^{123}I]IBVM in MBq (mCi)	VATSBI
Healthy	19	M	C	1	approximately 333 (9.00)	8.14
Healthy	21	M	C	1	344.1 (9.30)	5.88
Healthy	27	F	A	1	268.99 (7.27)	6.47
Healthy	28	M	A	1	334.11 (9.03)	3.66
Healthy	31	F	AA	0	280.83 (7.59)	5.30
Healthy	32	F	AA	0	333 (9.00)	3.34
Healthy	33	F	AA	0	approximately 333 (9.00)	5.88
Healthy	34	F	C	1	approximately 333 (9.00)	6.96
Healthy	44	F	AA	1	340.4 (9.20)	missing[a]
Rett syndrome	19	F	AA	0	321.9 (8.70)	4.26
Rett syndrome	21	F	C	0	approximately 333 (9.00)	6.34
Rett syndrome	22	F	C	0	approximately 333 (9.00)	4.82
Rett syndrome	31	F	C	0	257.15 (6.95)	5.34

0 = no, 1 = yes; A = Asian; AA = African-American; C = Caucasian; F = female; M = male; VATSBI = Vesicular Acetylcholine Transporter Binding Site Index.

[a]Meaningful data was not obtained due to technical malfunction of the gamma counter.

Synapse. Author manuscript; available in PMC 2012 October 24.

Table II

Rate constants of reversibly binding radioligands estimated by mathematical modeling for healthy control participants who received intravenous injections of approximately 333 MBq (9 mCi) (−)-5-[^{123}I]iodobenzovesamicol ([^{123}I]IBVM)

Age in years	Striatal K_1	Striatal k_2	Striatal k_3	Cerebellar K_1	Cerebellar k_2	Cerebellar k_3
19	0.0196	0.0137	0.0062	0.0205	0.0489	0.0038
21	0.0233	0.0158	0.0176	0.0249	0.0348	0.0065
27	0.00097	0.0099	0.012	0.0011	0.037	0.006
28	0.0122	0.0174	0.0225	0.0121	0.0312	0.0064
34	*a*	*a*	*a*	*a*	*a*	*a*
44	*a*	*a*	*a*	*a*	*a*	*a*

[a]Technical problems prevented meaningful estimates of the constants.

Table III

Genetic and clinical characteristics of participants with Rett syndrome (RTT) who received single-photon emission-computed tomography (SPECT) of the brain for sixty (60) minutes, twenty-four (24) hours following the intravenous injection of approximately 333 MBq (9 mCi) (−)-5-[^{123}I]iodobenzovesamicol ([^{123}I]IBVM)

Age in years	MeCP2 mutation	X-inactivation	HCc	Walks[a]	Feeds self[b]	ADLS[c]	Medications	H[d]	R[d]	S[d]	Sc[d]
19	T158M	Random	54 (35%)	0	0	0	phenobarbital	1	2	1	1
21	R306C	Skewed	50 (<2%)	2	1	2	carbemazepine, valproic acid	0	0	1	1
22	R294X	Random	48.5 (<2%)	0	0	0	levetiracetam, valproic acid	0	2	1	3
31	R270X	Random	53.3 (10%)	1	1	1	fluoxetine	1	1	0	1

HCc = head circumference in centimeters with percentiles in parentheses; H = hyperventilation; R = rigidity; S = seizures; Sc = scoliosis;

[a] 0 = cannot walk; 1 = walks with assistance; 2 = walks without assistance

[b] 0 = cannot feed self; 1 = can feed self

[c] Scores on Activities of Daily Living Scale (ADLS)

0 = neither walks nor feeds self

1 = walks with assistance and feeds self

2 = walks without assistance and feeds self

[d] Scores for H, S, Sc, and R: 0 = none. 1 = mild. 2 = moderate, 3 = severe.

Table IV

Characteristics of healthy subjects who received single-photon emission-computed tomography (SPECT) of the brain for sixty (60) minutes, twenty-four (24) hours following the intravenous injection of approximately 333 MBq (9 mCi) (−)-5-[^{123}I]iodobenzovesamicol ([^{123}I]IBVM)

Diagnosis	Age in years	Sex	Ethnicity	Handedness	Smokes cigarettes
Healthy	19	M	C	right	0
Healthy	21	M	C	left	1
Healthy	27	F	A	right	0
Healthy	28	M	A	right	0
Healthy	31	F	AA	right	0
Healthy	32	F	AA	right	0
Healthy	33	F	AA	right	1
Healthy	34	F	C	left	0
Healthy	44	F	AA	missing	missing

0 = absent; 1 = present; A = Asian; AA = African-American; C = Caucasian; F = female; M = male.

Table V

Focal areas with decreased Vesicular Acetylcholine Transporter Binding Site Index (VATSBI) voxel-cerebellar ratios in four participants with Rett syndrome (RTT) who received single photon emission computed tomography (SPECT) of the brain for sixty (60) minutes, twenty-four (24) hours following the intravenous injection of approximately 333 MBq (9 mCi) (−)-5-[^{123}I]iodobenzovesamicol ([^{123}I]IBVM) (Figure 5)

XYZ coordinates of peak % change			% change	Volume (mL)	Description (Brodman area numbers)
Left hemisphere:					
−14	−78	34	42.4	7.1	Parieto-occipital junction (17,18,31)
−4	−34	−4	39.2	3.9	Superior colliculus
−38	−28	12	38.9	8.9	Insula-transverse temporal gyrus
−4	−40	66	34.7	1.2	Post-central gyrus (21)
Right hemisphere:					
12	−22	46	35.6	2.0	Cingulate gyrus (31)
52	12	−12	34.2	2.6	Superior temporal gyrus (38)